The Flattened Face of Type IIβ Phosphatidylinositol Phosphate Kinase Binds Acidic Phospholipid Membranes†

Lisa M. Burden,‡,§ Vibha D. Rao,‡,§ Diana Murray,|| Rodolfo Ghirlando,‡ Scott D. Doughman,⊥ Richard A. Anderson,⊥ and James H. Hurley*,‡

Laboratory of Molecular Biology, National Institute of Diabetes and Digestive and Kidney Diseases, National Institutes of Health, Bethesda, Maryland 20892-0580, Department of Biochemistry and Molecular Biophysics, Columbia University, 630 West 168th Street, BB-221, New York, New York 10032, and Department of Pharmacology, University of Wisconsin Medical School, Madison, Wisconsin 53706

Received July 7, 1999; Revised Manuscript Received September 8, 1999

ABSTRACT: Type IIβ phosphatidylinositol phosphate kinase is a representative phosphatidylinositol phosphate kinase that is active against membrane-bound substrates. The structure of the enzyme contains a flattened basic face that spans the crystallographic dimer interface and is adjacent to the active site. Analytical ultracentrifugation shows that phosphatidylinositol phosphate kinase is a dimer in solution. Modeling suggested that the flattened face binds to acidic phospholipids by electrostatic interactions. The enzyme binds to acidic vesicles containing phosphatidylserine, phosphatidic acid, or phosphoinositides mixed with phosphatidylcholine, but not to neutral phosphatidylcholine vesicles. Binding to acidic vesicles is abolished in the presence of 1.0 M NaCl, consistent with an essential electrostatic contribution to the free energy of binding. The +14 charge on the flattened face of the dimer was reduced to +2 in the triple mutant Lys72Glu/Lys76Glu/Lys78Glu. The mutation has no effect on dimerization, but reduces the apparent K_A for 25% phosphatidylserine/75% phosphatidylcholine mixed vesicles by 16-fold. The reduction in the level of binding can be ascribed to a loss of electrostatic interactions based on the finite difference solution to the Poisson−Boltzmann equation. The mutant reduces catalytic activity toward phosphatidylinositol 5-phosphate by ∼50-fold. The wild-type enzyme binds half-maximally to phosphatidylinositol 4,5-bisphosphate-containing vesicles at a mole fraction of 0.3% in a phosphatidylcholine background, as compared to a 22% mole fraction in phosphatidylserine. The binding to phosphatidylinositol 4,5-bisphosphate-containing membranes is less sensitive to salt and to the triple mutation than binding to phosphatidylserine-containing membranes, suggesting that at least part of phosphatidylinositol 4,5-bisphosphate's interaction with the enzyme is independent of the flattened face. It is concluded that the flattened face of type IIβ phosphatidylinositol phosphate kinase binds to membranes through nonspecific interactions, and that this interaction is essential for efficient catalysis.

The phosphatidylinositol phosphate kinases (PIPKs)[1] are a family of lipid kinases that have a strong preference for membrane-bound phosphorylated phosphoinositide substrates (*1*−*6*). The PIPKs, also known as the PIPkins (*5*), are classified into types I and II, and each type is represented by three known isoforms, α, β, and γ. Type I PIPKs preferentially phosphorylate PI4P on the 5-hydroxyl, but are also capable of catalyzing several other phosphorylations (*7*−*9*). Type II PIPKs phosphorylate PI3P and PI5P on the 4-hydroxyl (*7*, *8*). The yeast PIPK homologue Fab1p phosphorylates PI3P on the 5-hydroxyl (*10*).

The structure of type IIβ PIPK (PIPKIIβ; *11*) revealed a remarkably flat 33 Å × 48 Å basic patch. We refer to this region as the "flattened face" because it appears to be squashed flat when compared to the structures of its distant cousins, the eukaryotic protein kinases (*11*, *12*). The structure suggested that PIPKIIβ carries out interfacial catalysis by presenting its flattened face flush with the bilayer surface. In this model, the flattened face contacts the phospholipid headgroups with little or no penetration into the lipid bilayer (*11*). This flounder-like mode of interfacial binding leads to a mechanism whereby the enzyme can phosphorylate its substrate in situ. It also suggests how the enzyme might effect an increased substrate affinity by coupling substrate binding to favorable protein−membrane interactions. Homologies between PIPKIIβ and other phosphoinositide kinases suggest the model, if correct, would hold for the rest of the PIPKs.

The PIPK surface interaction model is in sharp contrast to the membrane penetration exhibited by many other

† Supported in part by NIH Grants GM51968 and GM57549 to R.A.A., an American Heart Association predoctoral fellowship to S.D.D., and a Helen Hay Whitney fellowship to D.M.

* To whom correspondence should be addressed. Phone: (301) 402-4703. Fax: (301) 496-0201. E-mail: jh8e@nih.gov.

‡ National Institutes of Health.

§ These authors contributed equally to this work.

|| Columbia University.

⊥ University of Wisconsin Medical School.

[1] Abbreviations: PC, phosphatidylcholine; PS, phosphatidylserine; PIPKIIβ, type IIβ phosphatidylinositol phosphate kinase; PIP_2, phosphatidylinositol 4,5-bisphosphate; PI4P, phosphatidylinositol 4-phosphate; PI5P, phosphatidylinositol 5-phosphate; PI, phosphatidylinositol; PG, phosphatidylglycerol; PA, phosphatidic acid; [^{3}H]DPPC, [^{3}H]dipalmitoylphosphatidylcholine; BSA, bovine serum albumin; FDPB, finite difference Poisson−Boltzmann.

10.1021/bi991571a CCC: $18.00
Published on Web 10/23/1999

enzymes of lipid-mediated signal transduction (*13*). The protein kinase C homology C1 and C2 domains penetrate the membrane surface and make use of hydrophobic interactions to different degrees (*14*−*17*). Phospholipases A_2 ($sPLA_2$; *18*) and C (PLC; *19*) both insert into membranes by means of a hydrophobic rim about the active site. Annexins bind superficially to membrane surfaces as proposed for the PIPKs, but unlike the PIPKs, they do so via a Ca^{2+}-dependent bridge (*20*). These membrane binding mechanisms were inferred originally from crystal structures, but established by subsequent mutational analysis. Because the model for the PIPK−membrane interaction is so unusual, and because of its potentially wide implications for other phosphoinositide kinases, we set out to test this model by mutational analysis.

To validate the membrane interaction model and to study the determinants of the membrane binding, we used ultracentrifugation to assess the binding of PIPKIIβ to sucrose-loaded phospholipid vesicles, in conjunction with site-directed mutagenesis of the flattened face. We used sedimentation equilibrium centrifugation to determine whether changes in apparent binding caused by mutations were actually caused by changes in oligomeric structure. These data establish that both wild-type and mutant PIPK IIβ are dimers. PIPKIIβ has a net charge of +14 on its flattened face. In the study presented here, we have mutated three of the surface lysines to glutamates, to reduce the charge on the dimer by 12 units. Charge reversal mutagenesis has been used to study electrostatic interactions between membranes and several other peripheral binding proteins (*21*−*24*). The binding of wild-type and mutant PIPKIIβ to various phospholipids was evaluated so the role of electrostatics in binding of the basic patch to membrane vesicles containing acidic phospholipids could be addressed.

EXPERIMENTAL PROCEDURES

Materials. 1-Palmitoyl-2-oleoylphosphatidylserine, 1-palmitoyl-2-oleoylphosphatidylglycerol, 1-palmitoyl-2-oleoylphosphatidic acid, brain phosphatidylcholine, and plant phosphatidylinositol were purchased from Avanti Polar Lipids (Alabaster, AL). Phosphatidylinositol 4,5-bisphosphate (PIP_2) and phosphatidylinositol 4-phosphate (PI4P) both from bovine brain were purchased from Calbiochem, Inc. Phosphatidylinositol 5-phosphate (PI5P) was from Echelon, Inc. [^{3}H]Dipalmitoylphosphatidylcholine (DPPC; 80 Ci mmol^{-1}) was purchased from Amersham-Pharmacia. Membranes (100 nm) were from Avestin. Thrombin, bovine serum albumin (BSA), Expand DNA polymerase, and deoxynucleotides were from Boehringer Mannheim. All other chemicals were at least analytical grade. Primers were synthesized on an ABI DNA synthesizer. The pET28b vector was from Novagen, Inc. All restriction endonucleases and ligase were purchased from New England Biolabs. QIAquick gel extraction kits and DNA purification kits were from Qiagen, Inc. Resins chelating Sepharose and Affi-gel blue were from Pharmacia. Protein gels were from Novex, Inc.

Expression and Purification of Wild-Type and Mutant Enzymes. Wild-type human PIPKIIβ was expressed in *Escherichia coli* BL21 as an active hexahistidine fusion kinase (*25*) and purified on chelating Sepharose and Affi-gel blue columns as described previously (*11*). The triple lysine mutant was expressed and purified under the same conditions as the wild-type enzyme.

PIPKIIβ Membrane Binding Assay. The sucrose-loaded vesicle method was adopted, with minor modifications, from the procedure of Rebecchi, McLaughlin, and co-workers (*26*, *27*). Sucrose-loaded large unilamellar vesicles composed of various molar ratios (90:10, 85:15, 80:20, 75:25, 70:30, and 60:40) of phosphatidylcholine (PC) and phosphatidylserine (PS) and 75:25 PC/phosphatidylglycerol (PG), 87.5:12.5 PC/phosphatidic acid (PA), 75:25 PC/phosphatidylinositol (PI), 93.75:6.25 PC/PIP_2, and 91.7:8.3 PC/PIP were prepared. All mixtures contained a trace of [^{3}H]DPPC. These mixtures of lipids in chloroform were dried under a stream of nitrogen and suspended in a solution of 170 mM sucrose, 100 mM NaCl, and 20 mM Tris-HCl (pH 7.4). Aliquots of the 5 mM lipid suspension were subjected to five freeze−thaw cycles in liquid nitrogen. Lipids were extruded through a membrane with a 100 nm diameter pore size in a microextruder Liposofast (Avestin Inc., Ottawa, ON). The extruded lipids were diluted at least 2-fold with a solution containing 20 mM Tris-HCl (pH 7.4) and 100 mM NaCl and centrifuged at 45000*g* for 30 min at 22 °C (Beckman TL-100 centrifuge, TL100.1 rotor). The concentration of the lipid pellet was measured by counting the [^{3}H]DPPC using a liquid scintillation counter. The binding reaction was carried out by incubating 1 mM lipid with 500 nM PIPKIIβ and 200 nM BSA. The total bulk lipid concentration was 1 mM for all experiments. BSA was added to reduce the extent of nonspecific binding of the PIPKIIβ to tubes. The total reaction volume was 100 μL. The mixture was centrifuged at 45000*g* for 30 min at 22 °C. The top fraction of 75 μL was removed, and the volumes of the top and bottom fractions were adjusted to 100 μL by addition of assay buffer. All fractions were analyzed for their [^{3}H]DPPC counts and by SDS−polyacrylamide gel electrophoresis (4 to 20% Tris-glycine). Gels were silver stained. The densities of the bands were measured using a densitometer (Eagleeye-Stratagene). The vesicle-associated fraction of PIPKIIβ was calculated using the following formula:

$$A_v = [\beta A_b + (\beta - 1)A_t]/(\beta + \alpha - 1)$$

where A_b is the amount of PIPKIIβ in the bottom fraction and A_t is the amount in the top fraction of the suspension. α is the fraction of sedimented vesicles, and β is the fraction of total volume removed as supernatant. Assays with wild-type and mutant enzymes were carried out concurrently on the same vesicle preparations. Experiments for studying the electrostatic interaction of PIPKIIβ with membranes were carried out in the presence of 100 mM, 200 mM, 500 mM, and 1 M NaCl. The assay buffer used in the binding reactions was 20 mM Tris-HCl (pH 7.4), 10 mM DTT, 150 μg/mL PMSF, 5 μg/mL leupeptin, and the indicated amounts of NaCl.

Mutagenesis. The template for mutagenesis was the PIPKIIβ cDNA fragment encoding human PIPKIIβ subcloned into the *Nde*I and *Bam*HI sites of pET28b (Novagen, Inc.). Primers were synthesized using a 394 DNA/RNA synthesizer (ABI Applied Biosystems). To generate the triple lysine mutant, the coding region of PIPKIIβ was amplified in two PCRs using first the sense primer GGGAATTC-CATATGTCGTCCAACTGCACCAGCACCACG and the

antisense primer CAC**CTC**GAT**CTC**GCTGGAGGC**CTC**-GAAGTC and, separately, the sense primer GACTTC**GAG**-GCCTCCAGC**GAG**ATC**GAG**GTG and the antisense primer CGCGGATCCCTACGTCAGGATGTTGGACATAAACT-CGTT (mutated codons for Glu shown in bold). Amplification products were gel purified and included in a second reaction with the sense primer GGGAATTCCATAT-GTCGTCCAACTGCACCAGCACCACG and the antisense primer CGCGGATCCCTACGTCAGGATGTTGGACA-TAAACTCGTT. PCR was carried out using a GeneAmp PCR system (PE Applied Biosystems). The final amplification product was gel purified, digested with *Nde*I and *Bam*HI, and then ligated to a similarly digested and phosphatase-treated pET28b vector containing the PIPKIIβ gene. The entire sequence of the amplified product was verified by DNA sequencing.

Sedimentation Equilibrium Studies. Sedimentation equilibrium studies were conducted at 4.0 °C and three different rotor speeds, ranging from 8000 to 14 000 rpm, on a Beckman Optima XL-A analytical ultracentrifuge. Data were acquired as an average of 25 absorbance measurements at a nominal wavelength of 280 nm and a radial spacing of 0.001 cm. Equilibrium was achieved within 24 h. Samples of PIPKIIβ were dialyzed exhaustively against 0.5 M NaCl, 20 mM Tris (pH 8.0), 10 mM β-mercaptoethanol, and 1 mM EDTA at 4 °C prior to ultracentrifugation. Samples of the wild-type PIPKIIβ were loaded into the ultracentrifuge cells at nominal loading concentrations of 0.8, 0.5, and 0.3 A_{280}. Samples of the lysine mutant PIPKIIβ were studied at nominal loading concentrations of 1.0, 0.7, and 0.3 A_{280}.

Data were analyzed in terms of a single ideal solute to obtain the buoyant molecular mass, $M(1-\bar{\nu}\rho)$, using the Optima XL-A data analysis software (Beckman) running under Microcal Origin 3.78, by fitting data from each scan to $A_r = A_0 \exp[HM(1-\bar{\nu}\rho)(r^2 - r_0^2)] + E$, where A_0 is the absorbance at a reference point r_0, A_r is the absorbance at a given radial position r, H represents $\omega^2/2RT$, ω is the angular speed in radians per second, R is the gas constant, T is the absolute temperature, and E is a small baseline correction determined experimentally by collecting data at 42 000 rpm. Residuals were calculated. Values of M were obtained from the buoyant molecular mass, $M(1-\bar{\nu}\rho)$, and using densities, ρ, at 4 °C obtained from standard tables. A value of the partial specific volume $\bar{\nu}$ of 0.7358 mL/g was calculated for PIPKIIβ on the basis of the amino acid composition using the consensus data for the partial specific molar volumes of amino acids published by Perkins (*28*).

Protein and Membrane Models for Electrostatic Calculations. The PIPKIIβ dimer and the lipid bilayer were represented in atomic detail, and the solvent was modeled as a homogeneous medium with a constant dielectric. Via determination of the nonlinear Poisson−Boltzmann equation in the finite difference approximation (FDPB) (*29*), the electrostatic interaction between PIPKIIβ and PC/PS membranes was calculated as a function of the mole fraction of PS in the membrane, the ionic strength of the solution, and the net charge of the protein. The model is similar to the one used in the past in successfully analyzing the membrane binding of basic peptides and proteins (*30*−*33*).

Six different lipid bilayers (1:0, 8:1, 5:1, 3:1, 2:1, and 1:1 PC/PS) were created as described in ref *34*. The structure of the PIPKIIβ dimer was used to represent the enzyme minus the activation loop. Hydrogens were added to the wild-type structure using the program CHARMM (*35*). The model for the triple charge mutant was constructed by manually removing the side chains of the mutated Lys residues and using CHARMM to build Glu side chains in their place. The activation loop, disordered in the structure determination, was modeled as an amphipathic α-helix based on the strong helical propensity of this region predicted by the program PHD (*36*). The helical model was built and energy minimized using the Insight Biopolymer and Discover molecular modeling packages (INSIGHT-II, Biosym Technologies). The N- to C-terminal length of the activation loop model is 36 Å, significantly longer than the 22 Å distance it would have to span in the PIPKIIβ structure; hence, some adjustments to the ends of the helix would be required to fit into the intact enzyme.

No attempt was made to model the activation loop as part of the enzyme structure. Instead, the electrostatic interaction free energy of the full enzyme with membrane was approximated by considering separately the experimentally determined portion of the structure and the activation loop model, and then summing their individual contributions. Previous work showed the relative level of binding can be determined by considering a single orientation of the protein with respect to the membrane, specifically, the orientation of a minimum free energy in which the protein's potential interacts maximally with the membrane potential (*30*, *31*, *33*). In each calculation, the enzyme or the activation loop helix was placed in its most attractive orientation, ∼3 Å from the membrane surface; the enzyme was positioned with its basic flattened face parallel to the membrane surface, and the activation loop helix was positioned so that most of its basic residues point toward the membrane surface.

Finite Difference Poisson−Boltzmann Calculations. Each atom of the protein and membrane is assigned a radius and partial charge that is centered at its nucleus; the protein and membrane model is then mapped onto a three-dimensional lattice of l^3 points, each of which represents a small region of the protein, membrane, or solvent. Regions representing the molecules are assigned a dielectric constant of 2, and regions representing the surrounding aqueous phase are assigned a dielectric constant of 80. The charges and radii used for the amino acids were taken from a CHARMM22 parameter set (*35*); those used for the lipids are the ones described in ref *34* and used in previous studies (*30*, *31*, *33*). The electrostatic potential and the mean distribution of the monovalent salt ions at each lattice point are calculated by solving numerically the nonlinear Poisson−Boltzmann equation as described previously (*31*). The electrostatic potential due to the protein and the membrane when they are far apart and when they are close together are used to calculate the change in electrostatic free energy as the protein approaches the membrane (*37*). Calculations were performed on lattices with an l of 145 (for the activation loop model) and an l of 241 (for the PIPKIIβ structure) with focusing boundary conditions to final spatial resolutions of 2.0 and 1.6 grid spacings/Å, respectively. The electrostatic free energies of interaction from these calculations are estimated to be accurate to within 0.25 kcal/mol.

PIPK Activity Assay. Wild-type and mutant recombinant PIPKIIβ (2 μg in 50 μL reaction mixtures) were assayed in the presence of 50 mM Tris (pH 7.6), 10 mM $MgCl_2$, and

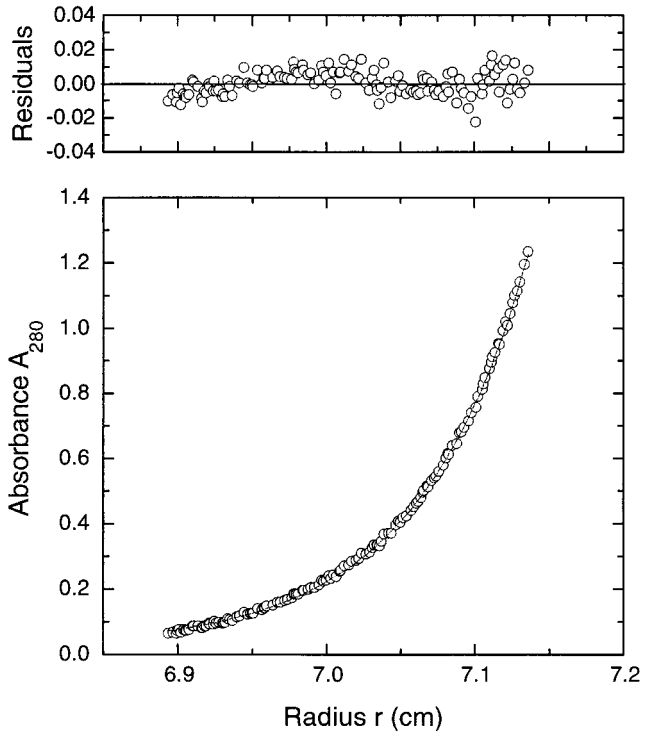

FIGURE 1: Triple lysine mutant PIPKIIβ exists as single, monodisperse dimers. Sedimentation equilibrium profile at 280 nm shown as a distribution of A_{280} at equilibrium. Data points were from a 12 000 rpm run at 4 °C. The results were analyzed for the best single-component $M(1-\bar{\nu}\rho)$ fit, shown as a line through the experimental points. The corresponding distribution of the residuals is shown above the plot.

0.5 mM EGTA with 5−50 μM PI5P substrate prepared in isotonic KCl solution, and 50 μM ATP spiked with 10 μCi of [γ-^{32}P]ATP (3000 Ci/mmol). The reactions were performed in duplicate at 37 °C for 5 min and then stopped by addition of 100 μL of 1 N HCl. The lipid products were extracted using 200 μL of chloroform/methanol (1:1). The organic phase was washed once in 100 μL of methanol/1 N HCl (1:1), and then spotted on TLC plates and run as described previously (*38*). After analysis by phosphoimaging (Molecular Dynamics; exposure time of 2 h), the PI(4,5)P_2 spots on the TLC plates were quantitated against the radioactivity used in the assays.

RESULTS

Sedimentation Equilibrium. To determine the oligomeric state of the wild-type and mutant PIPKIIβ, sedimentation equilibrium experiments were performed at various rotor speeds and different protein loading concentrations. Studies on the wild-type enzyme at rotor speeds of 10 000, 12 000, and 14 000 rpm led to identical values of $M(1-\bar{\nu}\rho)$, within the experimental precision of the method. The values of $M(1-\bar{\nu}\rho)$, averaged at 25 500 ± 1500 g/mol, showed no dependence on the loading concentration, confirming the observation that the samples were monodisperse. The experimentally obtained value of $M(1-\bar{\nu}\rho)$ corresponds to a measured molecular mass of 102 300 ± 6000 g/mol, indicating that under these conditions the protein is dimeric ($n = 2.16 \pm 0.13$).

The mutant enzyme was also found to be monodisperse and dimeric under similar conditions (Figure 1). The average

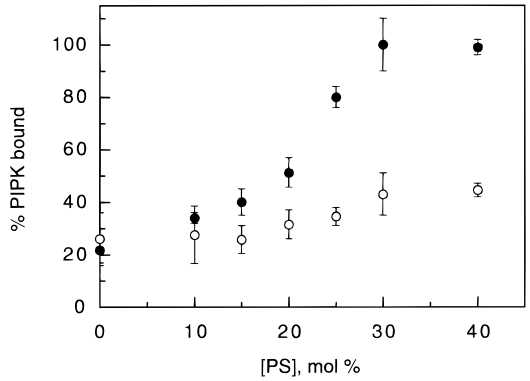

FIGURE 2: Effect of increasing membrane negative charge density on wild-type (●) and mutant (○) PIPKIIβ's binding to sucrose-loaded PC/PS vesicles. Data are expressed as averages ± standard deviations of three separate experiments performed in duplicate.

$M(1-\bar{\nu}\rho)$ value of 27 300 ± 1100 g/mol determined experimentally at rotor speeds of 8000, 10 000, and 12 000 rpm corresponds to a molecular mass of 109 600 ± 4500 g/mol ($n = 2.31 \pm 0.1$). The calculated value for the partial specific volume, ν, leads to dimer molecular masses that are 10−15% larger than the calculated values. When the fact that the value of the buoyant molecular mass does not depend on the rotor speed and loading concentration is considered, reversible higher-order equilibria with K_d values corresponding to the loading concentrations are ruled out. Contamination with an irreversible PIPKIIβ aggregate or a smaller than calculated experimental value for ν may contribute to the larger than expected dimer molecular mass.

Membrane Binding Properties of the Wild-Type Enzyme. The in vitro binding of wild-type PIPKIIβ to phospholipid vesicles was characterized. In the absence of lipids, 20% of the wild-type enzyme consistently sedimented in the pellet fraction, regardless of the freshness of the enzyme preparation or other experimental parameters that were tested. In the presence of the neutral lipid, phosphatidylcholine, the wild-type enzyme exhibited no significant binding to the vesicles (Figure 2). The 20% binding to PC vesicles is equal to the baseline sedimentation in the absence of lipids. An increase in concentration of PS led to an increased level of binding to the PC/PS vesicles. At 20 mol % PS, 50% of the enzyme is bound to the vesicles and the binding reaches a saturation at 30 mol % PS.

To test the effect of other negatively charged lipids, we studied the binding to vesicles containing PA, PG, PI, PI4P, and PIP_2. At pH 7.4, these lipids have negative charges of approximately −2, −1, −1, −3, and −4, respectively (*39*). To keep the total negative charge of the vesicles equal to that of 25 mol % PS, experiments were carried out at concentrations of 12.5 mol % phosphatidic acid, 25 mol % phosphatidylglycerol, 25 mol % phosphatidylinositol, 8.3 mol % PI4P, and 6.25 mol % PIP_2 (Figure 3a). Fifty percent of the enzyme was bound to PC/PI, and 75% bound in the case of PC/PA. In comparison, 85% of the protein was bound to PC/PS. For vesicles containing PI4P and PIP_2, PIPKIIβ was completely bound. Binding to these phosphoinositides is stronger than binding to other acidic lipids. For example, saturated binding occurs at a mole fraction of less than 1% PIP_2 (Figures 3b and 4). At a constant charge, replacement of phosphoinositides with PS leads to a marked reduction in the level of binding (Figures 3b and 4).

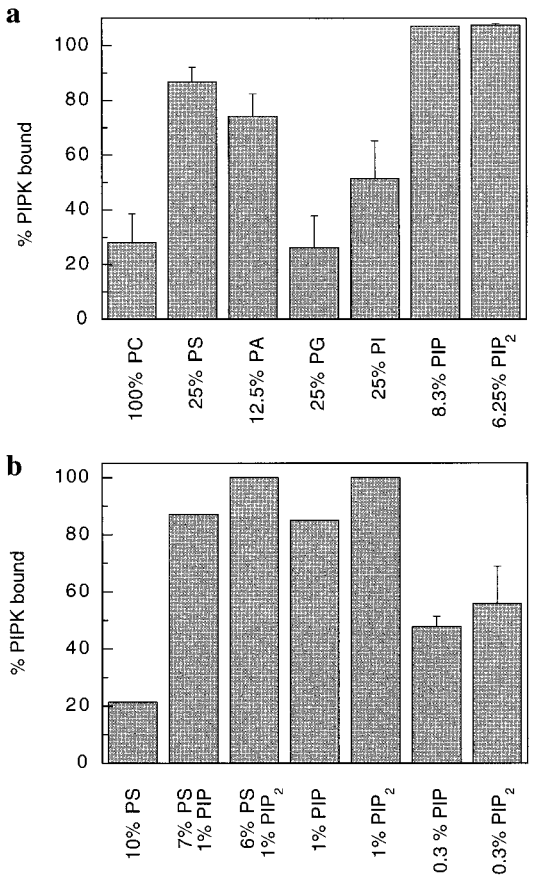

FIGURE 3: Histograms of the percentage of wild-type PIPKIIβ associated with vesicles containing various anionic lipids. (a) Vesicles have equal negative charge densities with the indicated lipid composition. Each bar represents the mean ± the standard error of the mean of five independent measurements, except the PI4P experiment which was carried out once and the PIP_2 experiment which was carried out twice. (b) Effect of doping PS-containing vesicles with 1% phosphoinositide while maintaining a constant negative surface charge. For comparison, measurements of PIPKIIβ binding to 0.3% and 1% phosphoinositide [PI4P or PIP_2] are included. Binding to 0.3% phosphoinositide is reported as the average of two measurements, while others are from single measurements.

Binding to acidic phospholipids is screened by increasing ionic strength. At a concentration of 25 mol % PS, an increase in the concentration of NaCl from 0.1 to 1.0 M reduces the level of binding of the enzyme to PS/PC vesicles from 80% to baseline (Figure 5). Binding to PI4P and PIP_2 decreases to near baseline at 1.0 M NaCl, but the level of binding at intermediate NaCl concentrations is greater than that for PS (Figure 5).

Design and Binding Properties of the Triple Lysine → Glutamate Mutant. The basic patch of PIPKIIβ was altered by mutating three of the lysines (K72, K76, and K78) to glutamates. This mutant was designed to eliminate the net positive charge on the surface of the molecule. The net change in charge of −6 per monomer drastically alters the basic nature of the flat face of the molecule (Figure 6). There is a single flattened face per dimer that spans the dimer interface. We have now verified that the enzyme is a dimer in solution as well as in the crystal. The mutation therefore changes the charge on a single flattened face by −12.

The mutation led to a disruption in acidic phospholipid binding without otherwise affecting the sedimentation behavior of the mutant protein. The amount of mutant enzyme that pelleted in the absence of vesicles and that bound to PC vesicles was equal to the baseline observed for the wild-type enzyme. However, the mutant has a much lower affinity for PC/PS vesicles than does the wild-type enzyme. At 40 mol % phosphatidylserine, while the wild-type enzyme exhibited saturated binding, less than 50% of the mutant was bound to the vesicles (Figure 2). The mutant also exhibited a reduced level of binding to vesicles containing low mole fractions of phosphoinositides, although the reduction was not as sharp as that seen for PS (Figure 4).

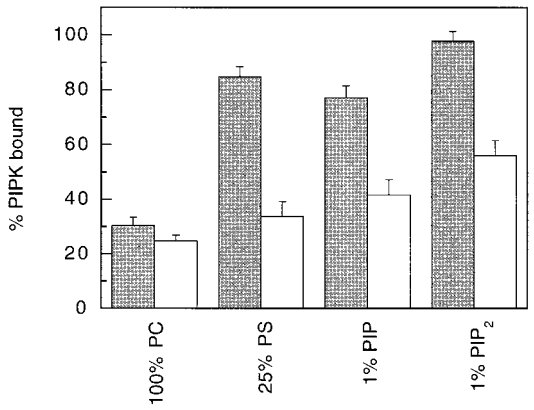

FIGURE 4: Binding of wild-type (gray bars) and mutant (white bars) PIPKIIβ to vesicles of pure PC or PC with the indicated amount of anionic phospholipid. Bars represent the mean ± the standard error of the mean of at least four but as many as eight separate measurements.

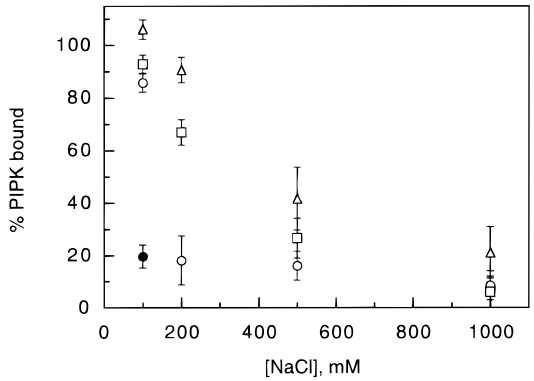

FIGURE 5: Effect of NaCl on the interaction of PIPKIIβ with the membrane. An increase in the concentration of NaCl screens the binding of the enzyme to mixed vesicles: PC (●), 25% PS (○), 1% PI4P (□), and 1% PIP_2 (△), all in a background of PC.

Theoretical Calculations. Following previous theoretical work on the membrane partitioning of basic peptides and proteins onto phospholipid bilayers (*30*, *31*, *33*), we calculated the electrostatic free energy of interaction of PIPKIIβ with phospholipid membranes as a function of the mole fraction of acidic lipid, the net charge of the protein, and the ionic strength of the solution. In our calculations, the enzyme was positioned with its basic flattened face oriented toward the membrane surface. Figure 7a shows the minimal electrostatic free energy of interaction between wild-type or mutant PIPKIIβ and PC/PS membranes as a function of the mole fraction of PS in 100 mM KCl. The model predicts the level of membrane partitioning of the wild-type enzyme increases strongly as the mole fraction of acidic lipid increases. In contrast, the overall electrostatic interaction is

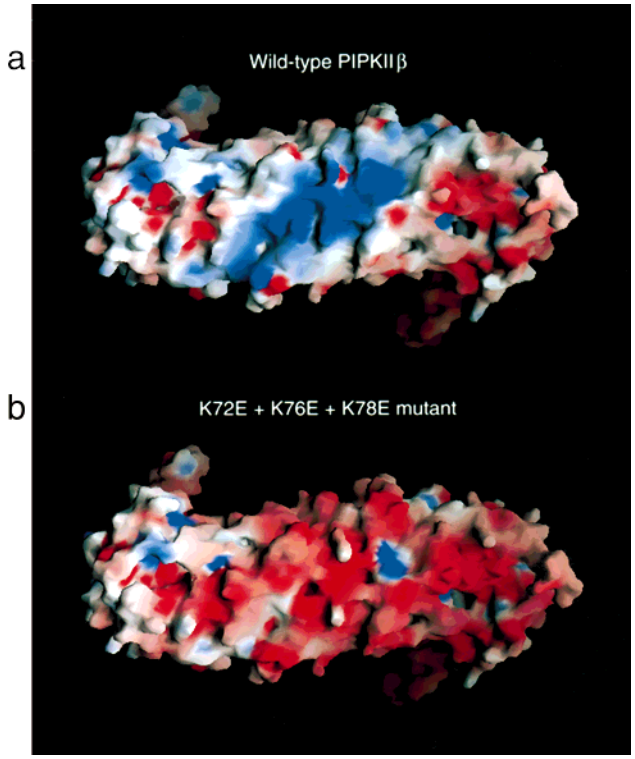

FIGURE 6: (a) Molecular surface of the PIPKIIβ dimer colored according to electrostatic potential using Grasp (*52*). (b) Surface of the triple lysine mutant. Saturating red indicates a ϕ of less than -10 *kT*/e, and saturating blue indicates a ϕ of more than 10 *kT*/e, where $T = 293$ K.

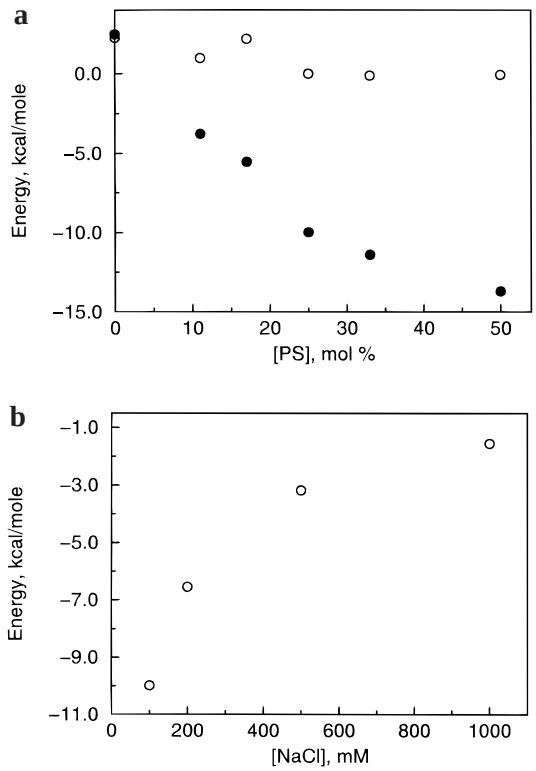

FIGURE 7: (a) Calculated interaction energies between wild-type (●) and mutant (○) PIPKIIβ and model membranes of various PC/PS compositions, as a function of PS mole fraction. (b) Interaction between wild-type PIPKIIβ and model membrane (25% PS) as a function of NaCl concentration.

predicted to be insignificant or even repulsive for the membrane partitioning of the charge reversal mutant. Figure 7b shows the minimal electrostatic free energy of interaction between wild-type PIPKIIβ and a 3:1 PC/PS membrane as a function of ionic strength. The model predicts that increasing the ionic strength of the solution greatly attenuates the electrostatic attraction between the enzyme and membrane and weakens the membrane partitioning. Overall, our calculations are consistent with the experimental observations which indicate PIPKIIβ interacts electrostatically with acidic phospholipids through its flattened face.

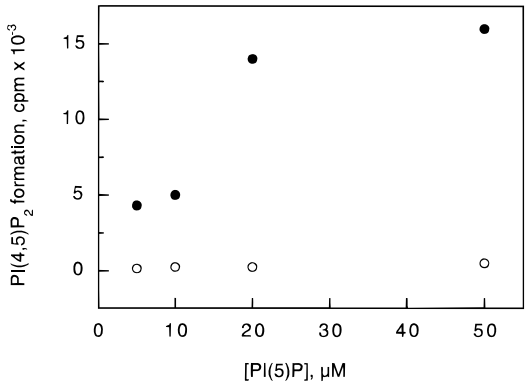

FIGURE 8: Enzyme activity of wild-type (●) and mutant (○) PIPKIIβ.

Enzyme Activity. Catalysis of PIP_2 formation from PI5P was assessed for wild-type and mutant enzymes (Figure 8). Both wild-type and mutant enzymes exhibit PI5P concentration-dependent activity, but the activity of the mutant is sharply reduced as compared to that of the wild type. The activity curve of the wild-type, but not the mutant, enzyme exhibits an inflection point at $\sim$15 μM PI5P. The activity of the mutant was so low that no effort was made to carry out a detailed analysis of substrate specificity.

DISCUSSION

Dimerization of PIPKIIβ. The major goal of this study was to determine whether the flattened face of PIPKIIβ is a membrane attachment site, as the crystal structure suggests. To answer this question, we compared the binding of wild-type and K72E/K76E/K78E PIPKIIβ to acidic phospholipid vesicles. This mutation was designed to reduce the total charge on PIPKIIβ by 12 units, assuming that the crystallographic dimer was preserved in solution. The first step in validating the model was to confirm that wild-type and mutant PIPKs are dimers in solution.

Wild-type and mutant PIPKIIβ are both dimers in solutions as determined by sedimentation equilibration in the analytical ultracentrifuge. These observations are consistent with the observed crystallographic dimer and with the structural integrity of the mutant protein. They are also consistent with previous gel filtration chromatography results that demonstrated oligomerization of erythrocyte PIPKII (*40*, *41*). This confirms that the triple mutation did not perturb the oligomeric structure of PIPKIIβ.

Membrane Attachment by the Flattened Face. We characterized the binding of wild-type PIPKIIβ to zwitterionic and anionic lipid vesicles to establish a basis for comparison to the mutant. No in vitro lipid binding studies of PIPKs have been reported until now. Wild-type PIPKIIβ does not bind to neutral PC vesicles. Wild-type PIPKIIβ was completely bound to PC/PS vesicles at a PS mole fraction of

$\geq$30%, a bulk lipid concentration of 1 mM, and an ionic strength of $\leq$100 mM.

Like wild-type PIPKIIβ, the mutant does not bind to PC vesicles. In contrast to the wild type, the mutant PIPKIIβ bound with sharply reduced affinity to PC/PS vesicles under otherwise identical conditions. The mutant was less than half bound to PC/PS vesicles at a PS mole fraction of 40%, the highest tested. The overall structural integrity and dimerization of the PIPKIIβ were not altered by the mutation as judged by its similar elution pattern on Affi-gel blue affinity chromatography and identical sedimentation in the analytical ultracentrifuge. Pending the structure determination of the mutant, we cannot rule out minor structural changes, but it seems unlikely that they could have a large enough effect to alter membrane binding at a remote site. The Debye length under the conditions used is roughly 8 Å, 1 order of magnitude smaller than the length of the PIPKIIβ dimer. Therefore, the charge reversal mutant could not have such a large effect on electrostatic interactions with the membrane if the mutation sites were distant from a membrane binding site. The only reasonable explanation remaining for the loss of binding is that the introduced negative charges come close enough to the membrane to directly repel it.

Electrostatic Interactions in Binding. To determine to what extent the binding was mediated by electrostatic interactions, the effect of ionic strength was tested. Increasing the ionic strength completely blocks binding of PIPKIIβ to PC/PS vesicles (Figure 5), consistent with a primarily electrostatic interaction. To determine whether binding to PS was mediated by specific interactions with the PS headgroup, as opposed to nonspecific electrostatic interactions, binding to a variety of other anionic lipids was tested. PIPKIIβ bound to most other acidic phospholipids, arguing against a specific binding site for PS. Curiously, PIPKIIβ did not bind to the anionic lipid PG. The binding experiment was repeated with two different lots of PG, and the chemical integrity of the PG was verified by thin-layer chromatography (data not shown). We have no explanation at present for the absence of binding to PG. As a function of charge density, PIPKIIβ binds with approximately equal affinity to PS and PA, more weakly to PI, and more tightly to PI4P and PIP_2. These findings confirm that the principal mode of interaction between the enzyme and the PC/PS membrane is through electrostatic interactions.

Phosphoinositide Binding. During the course of analyzing nonspecific interactions between PIPKIIβ and acidic membranes, we discovered an apparently specific interaction with phosphoinositides. The interaction with PI4P and PIP_2 is $\sim$10-fold stronger than with the other acidic phospholipids as a function of surface charge density. Binding of wild-type PIPKIIβ to PC/PIP_2 vesicles is saturated at less than 1% mol % PIP_2. The K72E/K76E/K78E protein has a reduced affinity for PC/PIP_2 vesicles (Figure 4), but the effect is not as pronounced as the loss of binding to PC/PS vesicles. By the same token, binding to PI4P and PIP_2 is less sensitive to screening by salt than binding to PS (Figure 5). Binding comparisons made at a constant charge density (Figure 3a) rather than at a constant mole fraction indicate that the high affinity for PI4P and PIP_2 cannot be entirely explained by the greater negative charge on the phosphoinositides. Furthermore, when PC/PS mixtures are doped with a small amount of PIP_2 while maintaining constant charge by reducing the mole fraction of PS, the PIP_2-containing vesicles bound with markedly higher affinity (Figure 3b). The high affinity for PIP_2, and to a lesser degree, PI4P, suggests a specific binding site for phosphoinositides. Further binding analysis of the full range of phosphoinositides using well-defined synthetic short- and long-chain lipids will be important for a more precise understanding of this binding site.

The modest reduction in PIP_2 affinity by the mutation suggests that binding involves a combination of structurally specific and nonspecific electrostatic interactions. We hypothesize the triple mutation affects the nonspecific component but not the specific component of the interaction. It is possible that the specific effect of PIP_2 on PIPKIIβ membrane binding could be explained by local aggregation of PIP_2 molecules, but the strength of the effect does not support this. PIP_2 is the product of the enzyme reaction, and might therefore interact at the active site. PI4P is neither a substrate nor a product of the reaction, but it is similar enough that nonproductive binding at the active site might occur. The specific PIP_2 and PI4P binding could occur at the active site or some other site distinct from the flattened face.

Implications of the Membrane Binding Mechanism. Taken together with the crystal structure, the mutational and binding analysis clarifies the role of the flattened face of PIPKIIβ as an attachment site for the surface of acidic membrane bilayers. The PIPKIIβ membrane binding model is the starting point for a structural understanding of catalysis, specificity, and regulation of the larger class of homologous PIPKs. Unfortunately, direct determination of the membrane-bound structure of PIPKs by high-resolution structural techniques is not feasible as yet. The dynamics of the membrane preclude crystal structure determination, and the size of PIPKs precludes solution analysis by NMR. We are left with model-based mutational analysis as the most appropriate probe of these interactions. By confirming that the flattened face is directly involved in phospholipid binding, we have strongly validated a model that is one of the cornerstones of future research into the PIPK mechanism.

Having confirmed an in vitro function for the flattened face, we might ask what its physiological function is. The charge composition of the PC/PS vesicles used in the study is similar to that of the inner leaflet of the mammalian cell plasma membrane. It is tempting to make inferences for the targeting of PIPKs in vivo. Indeed, electrostatic interactions mediate protein−membrane interactions in vivo for MARCKS (*42*), AKAP79 (*43*), and phospholipase C-β1 (*44*), among other examples. In these systems, electrostatic interactions with the acidic phospholipids of the plasma membrane were shown to be required for cell membrane association and for functional signaling.

The accumulated data suggest that the basic residues on the PIPK flattened face are not a major determinant for subcellular localization. The possibility that PIPKIIβ is localized at the plasma membrane at least transiently under some conditions is expected on the basis of the report that PIPKIIβ associates with and is activated by the plasma membrane-localized p55 TNF receptor (*25*). However, direct observation of plasma membrane-localized PIPKIIβ has not been reported. PIPKIIβ has been reported instead to colocalize with nuclear speckles in fibroblasts (*45*). These speckles are involved in RNA processing and do not contain

membrane. The basic residues of PIPKIIβ's flattened face are well conserved in other PIPKIIs. PIPKIIγ localizes predominantly to the endoplasmic reticulum in fibroblasts (*46*). The yeast homologue of type I PIPK, Mss4p, has been directly observed at the plasma membrane, where it plays a critical role in regulating actin organization (*47*, *48*). Some of the positive charges on the flattened face of PIPKIIβ are conserved in Mss4p, but they are largely absent in the PIPKI isozymes. PIPKIα and PIPKIβ localize predominantly at the plasma membrane (*49*). The kinase core of PIPKIγ is capable of reorganizing actin in transfected cells, suggesting that its kinase core alone can localize at least in part to the plasma membrane without the aid of other regulatory PIPK domains (*50*).

Other regions of the kinase core are likely to be more important in subcellular targeting. The activation loop emerged as a prime candidate because it is membrane-proximal and its sequence is conserved among PIPK types with similar subcellular localization. Indeed, studies with activation loop chimeras strongly support a key role for the activation loop in targeting and substrate specificity (J. Kunz, M. P. Wilson, M. Kisseleva, J. H. Hurley, P. W. Majerus, and R. A. Anderson, manuscript submitted for publication). Similarly, Wymann and co-workers recently showed that the corresponding loop in PI3Kγ is a key determinant for lipid substrate specificity (*51*). A breakdown of the FDPB-calculated electrostatic potentials into contributions from the flattened face versus the activation loop predicts that the activation loop contributes more to binding energy than the flattened face.

The positive charge on the flattened face of PIPKIIβ has an important role in interfacial catalysis, as judged from the sharp loss in activity of the mutant relative to that of the wild type. The loss of catalytic activity in the mutant is more dramatic than the loss of binding (Figure 8). It is intriguing that the curve for the wild-type, but not the mutant, enzyme exhibits an inflection point at which the activity sharply increases. Because the lipid substrate was not presented in a state of well-defined structure, we are not sure whether the inflection point is due to a change in the aggregation state of the lipid or to cooperativity in the enzyme−lipid interaction. The curve for the mutant did not exhibit an inflection point at a PI5P concentration of up to 200 μM (data not shown). Quantitative comparisons between the mutational effects on binding and catalysis cannot be made with the data presented here, since binding to PI5P-containing vesicles was not tested. Despite its limited scope, the enzymatic characterization presented here leaves no doubt that there is a major role for the flattened face in catalysis. This crucial catalytic contribution seems sufficient to account for its physiological function.

The electrostatic component of the flattened face's membrane interaction is probably specialized to the type II PIPKs and perhaps to Mss4p, but seems less likely to hold for the type I PIPKs and Fab1p. Almost none of the key basic residues of the type II PIPK's flattened face are conserved in the type I PIPKs and Fab1p. Although we believe the type I PIPKs also present a flattened face to the membrane surface, the precise energetic nature of the interactions might depend more on hydrogen bonds or hydrophobic interactions, as opposed to electrostatic ones. Alternatively, modeling suggests the loss of basic residues in type I PIPKs at positions conserved in the type II PIPKs may be partially offset by the presence of other type I-specific basic residues elsewhere on the membrane-binding face of the type I PIPKs.

Summary. In summary, our results indicate that PIPKIIβ interacts electrostatically with acidic phospholipid vesicles through its flattened face. The flattened face is probably more important for substrate affinity than for subcellular targeting. We have also confirmed that PIPKIIβ is a dimer in solution, and discovered a phosphoinositide interaction with a site distinct from the flattened face. The flattened face, and presumably its orientation relative to the membrane, are conserved in all PIPKs. The electrostatic component of the flattened face's interaction is particular to a subset of PIPKs, including the PIPKIIs. By validating a central aspect of the structural model for PIPK−membrane interactions, we hope to have laid the groundwork for a more complete understanding of some of the key issues for future research: mechanism of interfacial catalysis, substrate specificity, and regulation of subcellular localization.

ACKNOWLEDGMENT

We thank Stuart McLaughlin and Alexandra Newton for discussions.

REFERENCES

1. Boronenkov, I. V., and Anderson, R. A. (1995) *J. Biol. Chem. 270*, 2881−2884.
2. Fruman, D. A., Meyers, R. E., and Cantley, L. C. (1998) *Annu. Rev. Biochem. 67*, 481−507.
3. Martin, T. J. F. (1998) *Annu. Rev. Cell Dev. Biol. 14*, 231−264.
4. Toker, A. (1998) *Curr. Opin. Cell Biol. 10*, 254−261.
5. Hinchliffe, K. A., Ciruela, A., and Irvine, R. F. (1998) *Biochim. Biophys. Acta 1436*, 87−104.
6. Anderson, R. A., Boronenkov, I. V., Doughman, S. D., Kunz, J. C., and Loijens, J. C. (1999) *J. Biol. Chem. 274*, 9907−9910.
7. Zhang, X., Loijens, J. C., Boronenkov, I. V., Parker, G. J., Norris, F. A., Thum, O., Prestwich, G. D., Majerus, P. W., and Anderson, R. A. (1997) *J. Biol. Chem. 272*, 17756−17761.
8. Rameh, L. E., Tolias, K. F., Duckworth, B. C., and Cantley, L. C. (1997) *Nature 390*, 192−196.
9. Tolias, K. F., Rameh, L. E., Ishihara, H., Shibasaki, Y., Chen, J., Prestwich, G. D., Cantley, L. C., and Carpenter, C. L. (1998) *J. Biol. Chem. 273*, 18040−18046.
10. Gary, J. D., Wurmser, A. E., Bonangelino, C. J., Weisman, L. S., and Emr, S. D. (1998) *J. Cell Biol. 143*, 65−79.
11. Rao, V. D., Misra, S., Boronenkov, I. V., Anderson, R. A., and Hurley, J. H. (1998) *Cell 94*, 826−839.
12. Carpenter, C. L., and Cantley, L. C. (1998) *Nat. Struct. Biol. 10*, 843−845.
13. Hurley, J. H., and Grobler, J. A. (1997) *Curr. Opin. Struct. Biol. 7*, 557−565.
14. Zhang, G., Kazanietz, M. G., Blumberg, P. M., and Hurley, J. H. (1995) *Cell 81*, 917−924.
15. Xu, R. X., Pawelczyk, T., Xia, T.-H., and Brown, S. C. (1997) *Biochemistry 36*, 10709−10717.
16. Perisic, O., Fong, S., Lynch, D. E., Bycroft, M., and Williams, R. L. (1998) *J. Biol. Chem. 273*, 1596−1604.
17. Nalefski, E. A., and Falke, J. J. (1998) *Biochemistry 37*, 17642−17650.
18. Lee, B.-I., Yoon, E. T., and Cho, W. (1996) *Biochemistry 35*, 4231−4240.
19. Ellis, M. V., James, S. R., Perisic, O., Downes, C. P., Williams, R. L., and Katan, M. (1998) *J. Biol. Chem. 273*, 11650−11659.
20. Swairjo, M. A., Concha, N. O., Kaetzel, M. A., Dedman, J. R., and Seaton, B. A. (1995) *Nat. Struct. Biol. 2*, 968−974.

21. Campos, B., Mo, Y. D., Mealy, T. R., Li, C. W., Swairjo, M. A., Balch, C., Head, J. F., Retzinger, G., Dedman, J. R., and Seaton, B. A. (1998) *Biochemistry 37*, 8004−8010.
22. Ghomashchi, F., Lin, Y., Hixon, M. S., Yu, B.-Z., Annand, R., Jain, M. K., and Gelb, M. H. (1998) *Biochemistry 37*, 6697−6710.
23. Snitko, Y., Koduri, R. S., Han, S. K., Othman, R., Baker, S. F., Molini, B. J., Wilton, D. C., Gelb, M. H., and Cho, W. (1997) *Biochemistry 36*, 14325−14333.
24. Edwards, A. S., and Newton, A. C. (1997) *Biochemistry 36*, 15615−15623.
25. Castellino, A. M., Parker, G. J., Boronenkov, I. V., Anderson, R. A., and Chao, M. V. (1997) *J. Biol. Chem. 272*, 5861−5870.
26. Rebecchi, M., Peterson, A., and McLaughlin, S. (1992) *Biochemistry 31*, 12742−12747.
27. Buser, C. A., and McLaughlin, S. (1998) *Methods Mol. Biol. 84*, 267−281.
28. Perkins, S. J. (1986) *Eur. J. Biochem. 15*, 169−180.
29. Ben-Tal, N., Honig, B., Miller, C., and McLaughlin, S. (1997) *Biophys. J. 73*, 1717−1727.
30. Ben-Tal, N., Honig, B., Peitzsch, R. M., Denisov, G., and McLaughlin, S. (1996) *Biophys. J. 71*, 561−575.
31. Brooks, B. R., Bruccoleri, R. E., Olafson, B. D., States, D. J., Swaminathan, S., and Karplus, M. (1983) *J. Comput. Chem. 4*, 187−217.
32. Honig, B. H., and Nicholls, A. (1995) *Science 268*, 1144−1149.
33. Murray, D., Ben-Tal, N., Honig, B., and McLaughlin, S. (1997) *Structure 5*, 985−989.
34. Murray, D., Hermida-Matsumoto, L., Buser, C. A., Tsang, J., Sigal, C., Ben-Tal, N., Honig, B., Resh, M. D., and McLaughlin, S. (1998) *Biochemistry 37*, 2145−2159.
35. Peitzsch, R. M., Eisenberg, M., Sharp, K. A., and McLaughlin, S. (1995) *Biophys. J. 68*, 729−738.
36. Rost, B. (1996) *Methods Enzymol. 266*, 523−539.
37. Sharp, K. A., and Honig, B. H. (1990) *J. Phys. Chem. 94*, 7684−7692.
38. Loijens, J. C., and Anderson, R. A. (1996) *J. Biol. Chem. 271*, 32937−32943.
39. van Paridon, P. A., de Kruijff, B., Ouwerkerk, R., and Wirtz, K. W. A. (1986) *Biochim. Biophys. Acta 877*, 216−219.
40. Ling, L. E., Schulz, J. T., and Cantley, L. C. (1989) *J. Biol. Chem. 264*, 5080−5088.
41. Bazenet, C. E., Ruano, A. R., Brockman, J. L., and Anderson, R. A. (1990) *J. Biol. Chem. 265*, 18012−18022.
42. McLaughlin, S., and Aderem, A. (1995) *Trends Biochem. Sci. 20*, 272−276.
43. Dell'Acqua, M. L., Faux, M. C., Thorburn, J., and Scott, J. D. (1998) *EMBO J. 17*, 2246−2260.
44. Kim, C. G., Park, D., and Rhee, S. G. (1996) *J. Biol. Chem. 271*, 21187−21192.
45. Boronenkov, I. V., Loijens, J. C., Umeda, M., and Anderson, R. A. (1998) *Mol. Biol. Cell 9*, 3547−3560.
46. Itoh, T., Ijuin, T., and Takenawa, T. (1998) *J. Biol. Chem. 273*, 20292−20299.
47. Shibasaki, Y., Ishihara, H., Kizuki, N., Asano, T., Oka, Y., and Yazaki, Y. (1997) *J. Biol. Chem. 272*, 7578−7581.
48. Homma, K., Terui, S., Minemura, M., Qadota, H., Anraku, Y., Kanaho, Y., and Ohya, Y. J. (1998) *J. Biol. Chem. 273*, 15779−15786.
49. Desrivieres, S., Cooke, F. T., Parker, P. J., and Hall, M. N. (1998) *J. Biol. Chem. 273*, 15787−15793.
50. Ishihara, H., Shibasaki, Y., Kizuki, N., Wada, T., Yazaki, Y., Asano, T., and Oka, Y. (1998) *J. Biol. Chem. 273*, 8741−8748.
51. Bondeva, T., Pirola, L., Bulgarelli-Leva, G., Rubio, I., Wetzker, R., and Wymann, M. P. (1998) *Science 282*, 293−296.
52. Nicholls, A., Sharp, K. A., and Honig, B. (1991) *Proteins 11*, 281−296.

BI991571A